SPECIAL SECTION: REGULAR PAPER

International Symposium on Imaging, Sensing, and Optical Memory (ISOM' 22), Sapporo, Japan

Batch recording of multiple SQAM signal and self-reference detection technique

Jun Igarashi[1] · Hironori Ito[1] · Satoshi Honma[1]

Abstract

The development of holographic data storage is expected as a next-generation large-capacity memory. The recording scheme of spatial quadrature amplitude modulated (SQAM) signal, whose amplitude and phase are individually modulated with multi-levels, is a promising technique to improve the recording density of the memory. In this paper, we propose a method to simultaneously record multiple SQAM signals with different angles in the holographic memory. We also propose a method to detect the amplitude and phase value of the SQAM signal from the interference intensity distribution formed by the two SQAM signals selectively reproduced from the memory. We evaluate the decoding accuracy when the multiple SQAM signals generated by the interleaved phase method are recorded and the two signals are extracted and readout numerically. We also give experimental result as proof of principle of the decoding process. In the end, we analyze the accuracy against multiple number of SQAM signals on a recording page.

Keywords Holographic memory · Complex amplitude · Spatial quadrature amplitude modulation · Interleaved phase method

1 Introduction

The amount of digital data generated is increasing year by year, and the total amount stored in data centers around the world is expected to reach 170 ZB by 2025 [1, 2]. In data centers, the consumption of enormous resources and labor associated with the replacement of recording media that have reached the end of their life has become a problem. Another issue is the high-power consumption. As of 2018, data centers are already estimated to consume 200-terawatt hours (TWh) per year, of about 1% of the world's electricity demand. Data center power usage is also projected to grow nearly 15-fold by 2030, accounting for 8% of projected global demand [3].

Under these circumstances, the development of storage devices with low power consumption, long life, and low cost is required. The development of holographic memory with a high recording density of 2 Tbit/inch^2 or higher, a high transmission rate of 500 Mbit/sec or higher, and a long life of more than 20 years is expected [4–7].

In recent years, the use of spatial quadrature amplitude modulation (SQAM) signals, in which the amplitude and phase are individually modulated in multi-levels, has been investigated to further improve recording density [8, 9]. One of them is a method using an optical setup in which two independent SLMs for intensity- and phase-modulation are cascaded via a 4-f optical setup [10]. It is possible to easily generate the arbitrary SQAM signals by modulating the amplitude and phase values of the optical signal of each pixel individually with the two SLMs. Another method using two phase-modulated SLMs connected in parallel by a beam splitter has been proposed [11]. Two-phase modulation beams reflected from the different SLMs are multiplexed by the beam splitter and synthesize the arbitrary complex amplitude signal.

As a method using only one SLM, a method for generating a desired complex amplitude signal using computer-generated holographic technique has been proposed [12–16].

✉ Satoshi Honma
    shonma@yamanashi.ac.jp

1   Interdisciplinary Graduate School of Medicine
    and Engineering, University of Yamanashi, 4-3-11 Takeda,
    Kofu 400-8511, Japan

By projecting the phase pattern corresponding to the interference pattern of the signal beam and the reference beam onto the SLM, the desired SQAM signal is generated. It is possible to construct the optical setup using a modulator; therefore, it is easy to adjust the position of the optical elements and to suppress the cost for constructing the setup. The interleaved phase method is a very useful and easy-to-use technique for generating SQAM signals using only one SLM, one lens, and one aperture filter. In the system proposed below, we use this method to generate signals that are recorded in holographic memory.

On the other hand, methods for detecting the reproduced SQAM signal are also investigated. Since the phase of the light wave cannot be detected directly by a camera, an optical interferometer is usually used. One of the representative methods is the holographic diversity interferometry [17]. Using a beam splitter and polarization beam splitters, the signal light and the reference light are each split into four, and the signal light and the reference light are combined on the camera devices with the phase difference of 0, $\pi/2$, π, and $3\pi/2$. The complex amplitude value of the signal light is calculated from the interference fringe intensity distribution by the phase shift method.

As another method proposed is the space division phase shift method [18]. Using a checkerboard-shaped phase filter with phases of 0 and π, the signal light is split into four and spatially arranged in parallel. A similar optical system is used to generate the split parallel reference beams. By adjusting the position of the phase filter, phase differences of 0, $\pi/2$, π, and $3\pi/2$ can be obtained between the four signal beams. By interfering the signal light and the reference light at the camera plane, we obtain four interference fringe intensity distributions required for the phase-shifting method by a camera. Both methods require a relatively complicated optical system with various optical elements, such as beam splitters and phase filters. As a result, the optical system becomes larger, and the vibration resistance deteriorates.

As a method without an optical interferometer, the Transport of Intensity Equation (TIE) method has been proposed [19, 20]. This method measures the phase of the signal light from multiple intensity distributions acquired by shifting the camera along the optical axis. Since no reference beam is required and fewer optical elements are used, the overall optical system is simple. On the other hand, it is necessary to take multiple images while moving the camera, so there is a problem that the phase cannot be detected in real time.

In this paper, as a method for detecting SQAM signals without using a complicated optical setup for the interferometer or mechanical moving parts for the camera device, we propose a signal detection method by self-interference of multiple SQAM signals, and a batch recording optimized for the proposed method. In this method, a spatial light modulator is used to generate a multiplexed SQAM signal in which multiple SQAM signals are superimposed, and this is recorded with a single shot. In addition, only two SQAM signals are selectively reproduced from the multiplexed SQAM signal, and the phase of the signal is detected from this interference intensity distribution. Since the phase can be detected from the interference intensity distribution between the recorded signal beams without the need for an external reference beam, it is expected that it is expected that the optical system will be simplified, and vibration resistance will be improved. In addition, the SQAM signal can be measured in a single shot without moving parts.

First, we describe the principle of batch recording of multiple SQAM signals. Second, we numerically evaluate the measurement accuracy of the SQAM signal by the interference fringe with the two signals selectively reproduced. Third, we experiment the selective readout of the SQAM signal and the measurement of the phase and amplitude value of the signal as proof of the principle. In the end, the numerical analysis evaluates the reproduction accuracy for multiplexing number of SQAM signals to one page.

2 Batch recording of multiple SQAM signal and signal detection by selectively readout and self-interference

2.1 Generation of multiple SQAM signal

The principle of multiple SQAM signal generation is described below. The schematic diagram is shown in Fig. 1. The amplitude and phase modulated ith SQAM signal $d_i(x, y)$ is defined by the following equation:

$$d_i(x, y) = A_i(x, y)\exp\left[j\phi_i(x, y)\right] \tag{1}$$

where $A_i(x, y)$ and $\phi_i(x, y)$ are the amplitude and phase values of $d_i(x, y)$, x, y are the horizontal and vertical coordinates of the SLM, and the subscript i is the signal number. The liner phase code $L_i(x, y)$ defined by the following equation is multiplied by each SQAM signal $d_i(x, y)$:

$$L_i(x, y) = \exp\left[jk\left(\theta_i^x x + \theta_i^y y\right)\right] \tag{2}$$

where $k = 2\pi/\lambda$ and λ are the wavenumber and wavelength of the light, and θ_i^x and θ_i^y are the linear phase coefficients in the x and y directions, respectively. The values of θ_i^x and θ_i^y are determined so that each component for $d_i(x, y)$ is focused at a different position in the Fourier plane. A recording page data $C(x, y)$ composed of multiple SQAM signals is given by

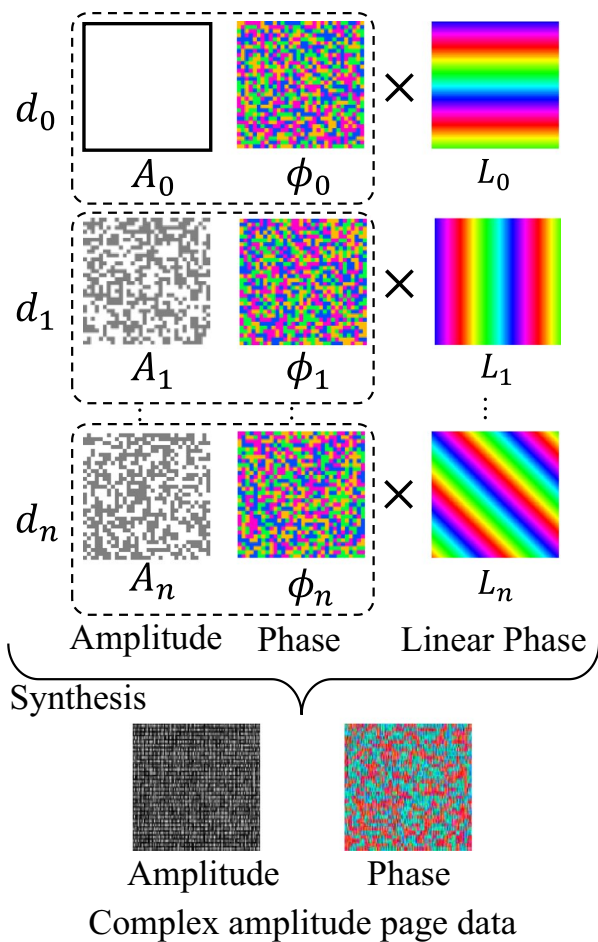$$C(x, y) = \sum_{i=0}^{n-1} d_i(x, y)L_i(x, y) \tag{3}$$

Fig. 1 Schematic diagram of the synthesis processing of a page data consisting of multiple SQAM signals

where $d_r(x, y)$, which is one of $d_i(x, y)$ is used for a self-reference signal and the amplitude value of it is constant and the phase value is determined to be a known value.

2.2 Batch recording of multiple SQAM signals

Figure 2 shows the optical system during recording. Based on the interleaved phase method, the phase distribution $P(x, y)$ corresponding to $C(x, y)$ is pre-calculated by

$$P(x, y) = \arg[C(x, y)] + (-1)^{\frac{x}{\Delta x}}(-1)^{\frac{y}{\Delta y}} \cos^{-1}[|C(x, y)|] \quad (4)$$

where $\arg\{C(x, y)\}$ is the phase value of $C(x, y)$, and Δx and Δy are the pixel pitches in the x- and y-directions of the SLM. We consider $(-1)^{\frac{x}{\Delta x}}(-1)^{\frac{y}{\Delta y}}$ as $(-1)^q(-1)^r$, where q and r are integers representing the number of pixels for the horizontal and vertical directions of the spatial modulator. SLM modulates the phase of light according to $P(x, y)$.

The complex amplitude value of the phase modulated light with $P(x, y)$ is given by

$$\exp\{jP(x, y)\} = \exp\{j \arg[C(x, y)]\}$$
$$\exp\{j(-1)^q(-1)^r \cos^{-1}(|C(x, y)|)\}$$
$$= \exp\{j \arg[C(x, y)]\} \cos\{\cos^{-1}(|C(x, y)|)\}$$
$$+ j(-1)^q(-1)^r \sin\{\cos^{-1}(|C(x, y)|)\}$$
$$= |C(x, y)| \exp\{j \arg[C(x, y)]\} + j(-1)^q(-1)^r$$
$$\sqrt{1 - |C(x, y)|^2} \exp\{j \arg[C(x, y)]\}$$
$$= C(x, y) + j(-1)^q(-1)^r \quad (5)$$
$$\sqrt{\frac{1 - |C(x, y)|^2}{|C(x, y)|^2}} C(x, y)$$
$$= \sum_{i=0}^{n-1} d_i(x, y)L_i(x, y) + j(-1)^q(-1)^r \sum_{i=0}^{n-1}$$
$$\sqrt{\frac{1 - |C(x, y)|^2}{|C(x, y)|^2}} d_i(x, y)L_i(x, y)$$

The equations imply that the phase modulation signal consists of the first term corresponds to SQAM page data, and the second term of an unnecessary component.

Here, we define $u_i(x, y)$ by

$$u_i(x, y) = j\frac{1}{4}\sqrt{\frac{1 - |C(x, y)|^2}{|C(x, y)|^2}} d_i(x, y) \quad (6)$$

and approximate $(-1)^q(-1)^r$ with

$$(-1)^q(-1)^r \approx \frac{1}{2}\left\{\exp\left[j\pi\left(\frac{x}{\Delta x}\right)\right] + \exp\left[-j\pi\left(\frac{x}{\Delta x}\right)\right]\right\}$$
$$\times \frac{1}{2}\left\{\exp\left[j\pi\left(\frac{y}{\Delta y}\right)\right] + \exp\left[j\pi\left(\frac{y}{\Delta y}\right)\right]\right\}. \quad (7)$$

Substituting Eqs. (6, 7) into the Eq. (5) gives the following equation:

$$\exp\{jP(x, y)\} = \sum_{i=0}^{n-1} d_i(x, y)L_i(x, y)$$
$$+ j\sum_{i=0}^{n-1} u_i(x, y)L_i(x, y)\left\{\exp\left[j\pi\left(\frac{x}{\Delta x}\right)\right] + \exp\left[-j\pi\left(\frac{x}{\Delta x}\right)\right]\right\} \quad (8)$$
$$\times \left\{\exp\left[j\pi\left(\frac{y}{\Delta y}\right)\right] + \exp\left[-j\pi\left(\frac{y}{\Delta y}\right)\right]\right\}$$

The phase-modulated beam is focused on the spatial filter by an object lens. The lens produces the Fourier transfer pattern of the input beam at its focal plane. The relationship between the distribution of the input beam $w(x, y)$ and the spectrum $S(x', y')$ at the focal plane is given by the following equation:

$$S(x', y') = \frac{\exp(jkf)}{j\lambda f} \int\int w(x, y) \exp\left\{-\frac{jk}{f}(xx' + yy')\right\} dxdy \quad (9)$$
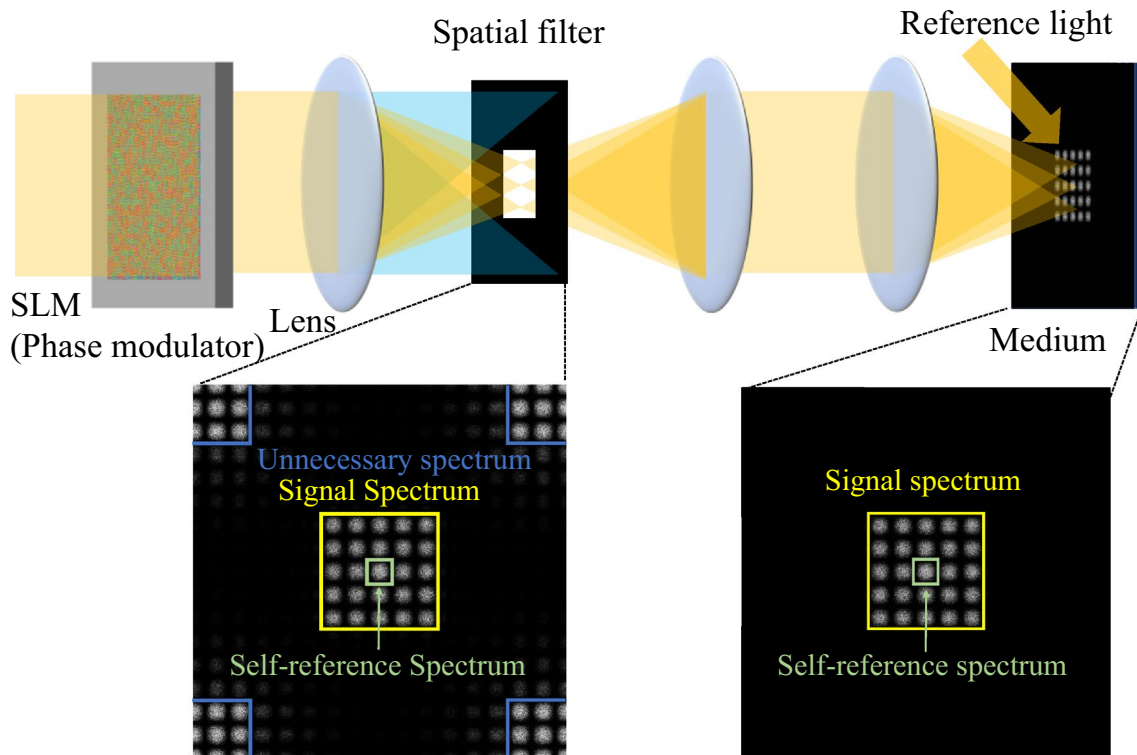
Fig. 2 Optical system for recording

where f is focal length of the lens, (x, y) indicate the coordinate on the SLM and (x', y') also indicate that on the focal plane. In the following, we rewrite the equation as $\mathcal{F}[u(x, y)]$.

The spatial distribution of the phase-modulated beam after the Fourier transform with the lens is given by

$$
\begin{aligned}
\mathcal{F}\left[\exp\{jP(x, y)\}\right] = &\sum_{i=0}^{n-1} D_i\left(x' - f\theta_i^x, y' - f\theta_i^y\right) \\
&+ \sum_{i=0}^{n-1}
\begin{Bmatrix}
U_i\left(x' + \frac{f\pi}{k\Delta x} - f\theta_i^x, y' + \frac{f\pi}{k\Delta y} - f\theta_i^y\right) + U_i\left(x' - \frac{f\pi}{k\Delta x} - f\theta_i^x, y' + \frac{f\pi}{k\Delta y} - f\theta_i^y\right) \\
+ U_i\left(x' - \frac{f\pi}{k\Delta x} - f\theta_i^x, y' + \frac{f\pi}{k\Delta y} - f\theta_i^y\right) + U_i\left(x' + \frac{f\pi}{k\Delta x} - f\theta_i^x, y' - \frac{f\pi}{k\Delta y} - f\theta_i^y\right)
\end{Bmatrix}
\end{aligned}
\tag{10}
$$

$D_i(x', y')$ and $U_i(x', y')$ are the Fourier transform of $A_i(x, y)$ and $u_i(x, y)$, respectively. We found that $D_i(x', y')$ and $U_i(x', y')$, which correspond to the spectra of the SQAM signal and the unnecessary component, are distributed around the position of $(x', y') = (f\theta_i^x, f\theta_i^y), (f\theta_i^x \pm \frac{f\pi}{k\Delta x}, f\theta_i^y \pm \frac{f\pi}{k\Delta y})$, respectively. Therefore, by adjusting the value of θ_i^x and θ_i^y, the spectrum of the each SQAM signal $D_i(x, y)$ can be arranged without spatial overlap. Unnecessary components $U_i(x', y')$ paired with $D_i(x', y')$ are distributed at positions $\pm\frac{f\pi}{k\Delta x}$ for x'-direction and $\pm\frac{f\pi}{k\Delta y}$ for y'-direction from the focus position of $D_i(x', y')$, respectively. Therefore, the spectrum of each SQAM signal and unnecessary components are spatially separated, and it is possible to remove the unnecessary component by spatial filtering.

As an example, the intensity distribution of the recording page data consisting of the 25 SQAM signals on the Fourier plane is shown in Fig. 2. The spectrum of each SQAM signal $D_i(x, y)$ is focused at slightly shifted positions on the recording plane, so that they do not overlap. The unnecessary components are distributed away from the position, where the signal is distributed.

After blocking the unnecessary spectrum with a spatial filter, the other components corresponding to SQAM signal
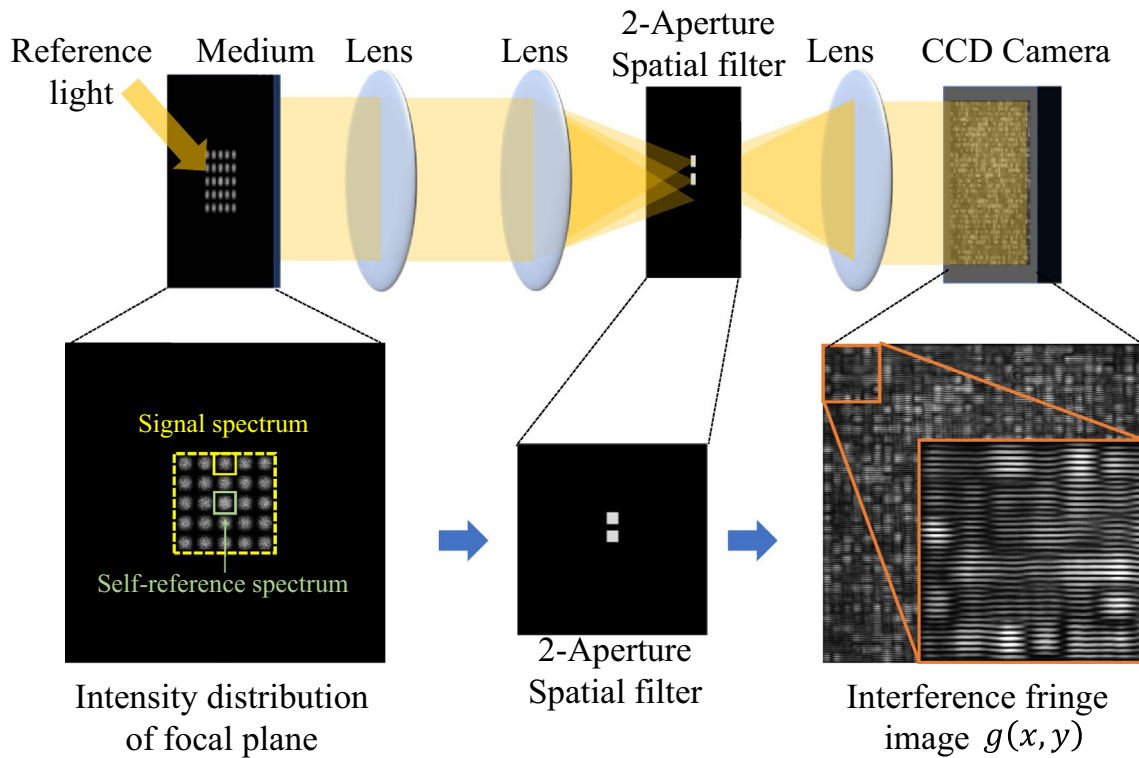
Fig. 3 Optical system for regeneration

$D_i(x, y)$ and the reference beam are irradiated onto the recording medium to record the hologram.

2.3 Reproduction of SQAM signals and phase detection with self-reference technique

Figure 3 shows the optical system for the regeneration process. A hologram is irradiated with a reference beam and all SQAM signals D_i are reconstructed. Then, the spectral distributions of the self-reference signal D_r and arbitrary signal light D_i are extracted simultaneously using a two-aperture spatial filter placed at the back of the recording medium. Each light passes through the lens. The interference fringes of the two lights are captured by the camera.

For simplicity of explanation, we consider only the x-direction. Assume that the amplitude and phase values of the self-reference beam are constant A_r and a known distribution $\varphi_r(x)$, respectively. We also assume the linear phase coefficient $\theta_r = 0$. The interference fringe intensity distribution $g(x)$ with one of SQAM signal $d_i(x)$ and self-reference signal $d_r(x)$ is given by

$$g(x) = \left| d_i(x)L_i(x) + d_r(x)L_r(x) \right|^2 \tag{11}$$

where the complex amplitude of the SQAM signal $d_i(x)$ and the linear phase code $L_i(x)$ are given by

$$d_i(x) = A_i(x)\exp(j\phi_i(x)) \tag{12}$$

and

$$L_i(x) = \exp\left\{jk\theta_i^x x\right\} \tag{13}$$

respectively from Eqs. (1) and (2). The values of the self-reference signal are also given by

$$d_r(x) = A_r\exp(j\phi_r(x)) \tag{14}$$

and

$$L_r(x) = 1. \tag{15}$$

The complex amplitude value $d_i(x)$ of the SQAM signal is investigated by applying the Fourier fringe analysis, whose process is described below, to the obtained interference intensity distribution [21]. Substituting Eqs. (12–15) into Eq. (11) and expanding it, the following equation is obtained:

$$\begin{aligned} g(x) = &A_i(x)^2 + A_r^2 + A_i(x)A_r \exp \\ &\left\{j\left\{\phi_i(x) - \phi_r(x)\right\}\right\} \exp\left\{jk\theta_i^x x\right\} \\ &+ A_i(x)A_r \exp\left\{-j\left\{\phi_i(x) - \phi_r(x)\right\}\right\} \\ &\exp\left\{-jk\theta_i^x x\right\} \end{aligned} \tag{16}$$

a, b, and b^* are defined by

$$a(x) = A_i(x)^2 + A_r^2 \tag{17}$$

$$b(x) = A_i(x)A_r\exp\{j\{\phi_i(x) - \phi_r(x)\}\} \tag{18}$$

$$b^*(x) = A_i(x)A_r\exp\{-j\{\phi_i(x) - \phi_r(x)\}\} \tag{19}$$

and then rewrite the Eq. (16) as

$$g(x) = a(x) + b(x)\exp\{jk\theta_i^x x\} + b^*(x)\exp\{-jk\theta_i^x x\} \tag{20}$$

Applying the Fourier transform to Eq. (20), we obtain

$$\mathcal{F}[g(x)] = A(x') + B(x' - f\theta_i^x) + B^*(x' + f\theta_i^x) \tag{21}$$

where $A(x')$, $B(x')$ and $B^*(x')$ are the Fourier transform value of $a(x)$, $b(x)$ and $b^*(x)$, respectively. We found that the above three components are distributed around $x' = 0$, $x' = f\theta_i^x$ and $x' = -f\theta_i^x$. By extracting the component $B(x' - f\theta_i^x)$ distributed around $x' = f\theta_i^x$ and shifting its position by $f\theta_i^x$ in opposite direction to x', we obtained the component $B(x')$. The appropriate range for extracting $B(x' - f\theta_i^x)$ depends on the resolution of the SQAM signal. The details of determining the range are explained in Chapter 3.

By performing the inverse Fourier transforming on $B(x')$,

$$b(x) = \mathcal{F}^{-1}[B(x')] \tag{22}$$

is obtained. Note that $b(x)$ corresponds to $A_i(x)A_r\exp\{j(\phi_i(x) - \phi_r(x))\}$ from Eq. (18). In this equation, A_r and $\phi_0(x)$ are the amplitude and phase distribution of the self-reference signal and the values are known. By dividing $b(x)$ by the complex value of $A_r\exp\{-j\phi_r(x)\}$,

it is possible to estimate the complex amplitude value of $d_i(x) = A_i(x)\exp\{j\phi_i(x)\}$.

3 Relationship between data resolution and area required for recording hologram

Figure 4 shows one of the SQAM signals included in the recording page data and the area on the recording medium required to record the signal. Several pixels of the spatial modulator must be used to generate a one-symbol of the complex-amplitude signal using the interleaved phase method. Assuming that the number of pixels used for the one-symbol is $Lp \times Lp$, the actual size of a symbol is given by

$$Lp\Delta x \times Lp\Delta y \tag{23}$$

where Δx and Δy are pixel pitch of SLM, and Lp is the number of pixels used in the x and y directions of the SLM. In this case, the effective pitch of the SQAM signal is $Lp\Delta x$ and $Lp\Delta y$ against x- and y-direction, and the area required to record a signal composed of above pixel pitch in Fourier space is derived from Eq. (9) by

$$\frac{2f\lambda}{Lp\Delta x} \times \frac{2f\lambda}{Lp\Delta y} \tag{24}$$

where the value corresponds to the area required to record the main lobe component of the Fourier-transformed distribution of the SQAM signal. According to the relationship between the actual size of a symbol in the SQAM signal and the required recording area from Eqs. (23) and (24), we found that reducing the area for a symbol improves the resolution of the SQAM signal and increases the amount of

Fig. 4 Relationship between resolution of SQAM signal and recording area. **a** Pixels of SLM used for 1 symbol of SQAM signal and **b** spectrum of SQAM signal

A SQAM signal included in a recording page data
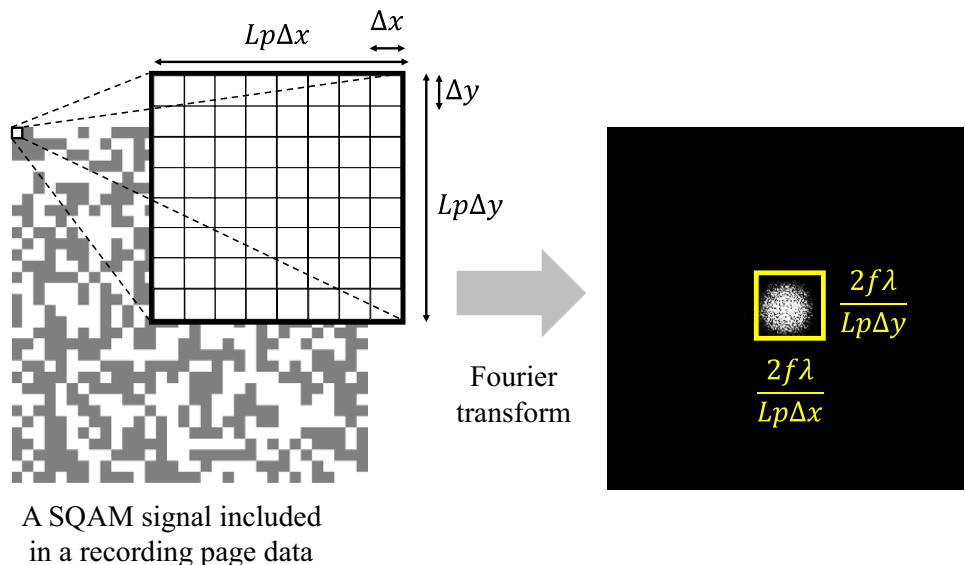
information, but the area on the recording medium required for recording becomes large. Therefore, there is a clear trade-off between the resolution of SQAM signals and the recording area, and the recording density for the information amount does not depend on the resolution of SQAM signals. This limitation also applies to recording signals composed of multiple SQAM signals.

To elaborate, let us assume that the maximum number of SQAM signals is bundled, and it is recorded on the medium under the condition that the signal components are arranged without overlapping and the unwanted component are spatially separated. Figure 5 shows one of the SQAM signals included in the recording page data and the exposure intensity of the recording signal on the medium, where the figure below shows the result of 1/4 times the area of one symbol of the SQAM signal. The resolution of

an SQAM signal is quadrupled, and as a result, the amount of information in an SQAM signal is also quadrupled. On the other hand, from the relationship of Eqs. (23) and (24), four times the recording area is required for each signal component to record a signal. Each signal component is irradiated onto the recording medium in a state of being arranged at regular intervals without overlapping. As the area required to record a signal component increases, the number of components that can be recorded in a given area decreases. Therefore, when recording multiple SQAM signals, the number of signals that can be recorded per the given area changes depending on the resolution of the SQAM signal, but if the recording area is the same, the amount of information recorded there is constant. Note that in the method proposed here, one of the multiplexed signals must be used as a self-reference signal. Considering this, when the number of bundle signals is reduced, the amount of recording information per area is reduced by that of for the self-reference signal, although it is small.
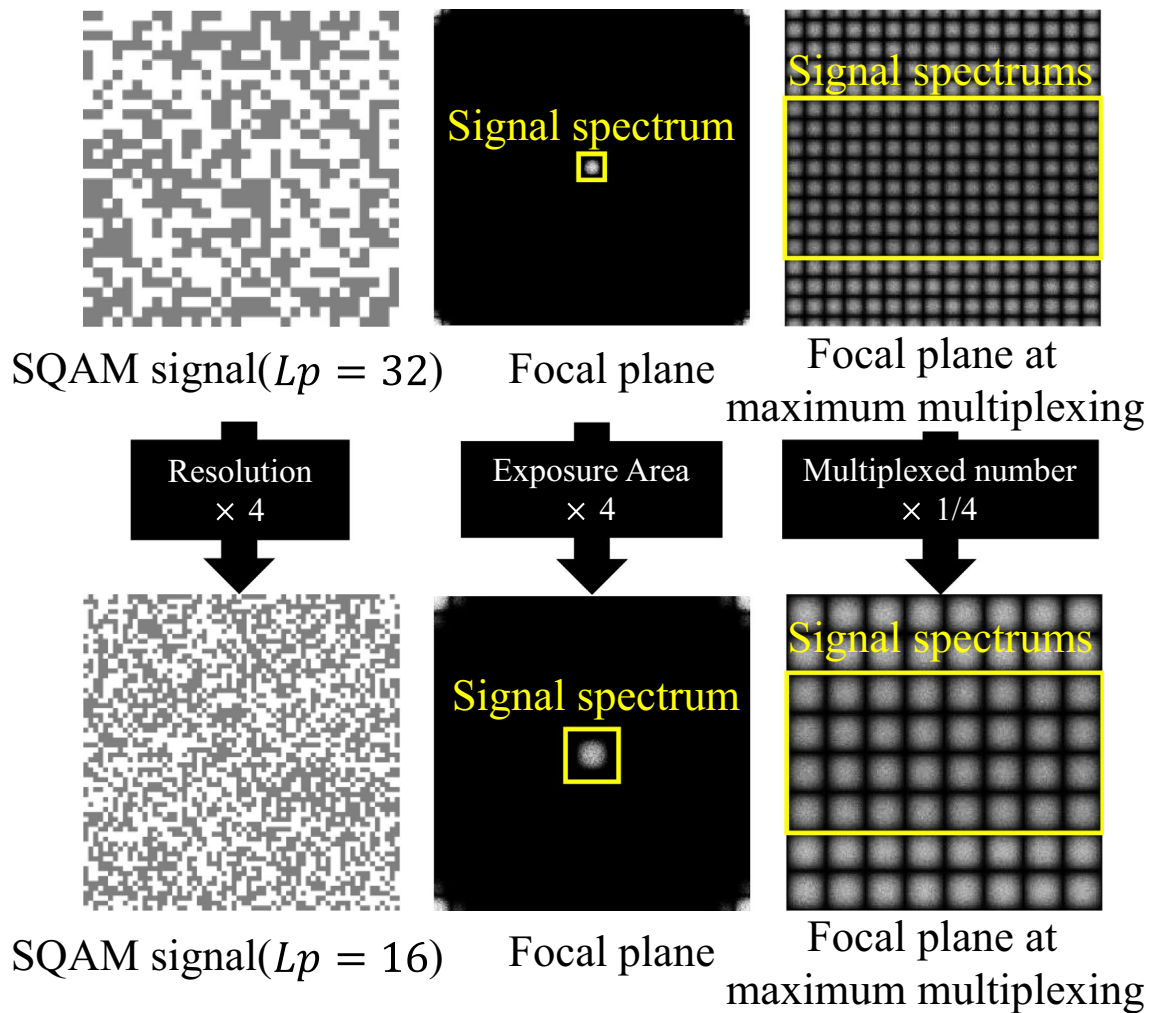

Fig. 5 Relationship of resolution of SQAM signals and exposure area on holographic memory

4 Numerical analysis of the reproduction accuracy of SQAM signals

The recording density relative to the amount of information is independent of the number of multiplexes of the SQAM signals. However, the effect of the pixel number used for a symbol Lp^2 on the symbol error ratio (SER) due to recording and reproduction of SQAM signals must be considered, where SER is defined as the ratio of the number of erroneous symbols to the total number of symbols. The reproduction accuracy of self-interference decoded SQAM signals was evaluated by numerical analysis. In the analysis, the amplitude and phase values of a symbol were modulated to 2 and 4 values, respectively, and the size of a symbol Lp was set to 16 and 32, 64, respectively. It was assumed that bundle SQAM page data $C(x, y)$ consisted of 9 SQAM signals generated by the interleaved phase method.

A phase codes is given, so that the spectrum of each SQAM signal is arranged in a 3×3 matrix in the x- and y-directions on the recording plane, as shown in Fig. 6. The spectrum of each SQAM signal does not overlap, where the spectrums are distributed around the position separated from each other by $\frac{2f\lambda}{Lp\Delta x}$ and $\frac{2f\lambda}{Lp\Delta y}$ in the x- and y-directions. The analysis conditions are listed in Table 1.

First, the bundle SQAM signal was Fourier transformed and the spectral distribution consisting of the nine components was calculated. This is assumed to be the signal recorded in the holographic memory and the signal to be reproduced later. The center SQAM signal component was used as the reference signal. At second, we extracted this and one of the other spectral components of the SQAM signal, where each component was extracted with a filter of size $\frac{2f\lambda}{Lp\Delta x} \times \frac{2f\lambda}{Lp\Delta y}$. The above two components were inverse Fourier transformed and the intensity distribution corresponding to the interference fringes captured by the

Table 1 Parameters for numerical analysis

Multiplexed number	9
Data number i	0~8
Bit per symbol	3
Lp	16, 32, 64
SLM pixels	1024×1024
Pixel pitch of SLM	10 μm
Focal length of lens f	10 mm
Wavelength λ	633 nm

camera were calculated. Finally, the SQAM signal was decoded using the Fourier fringe analysis described in Sect. 2.3.

The amplitude, phase, and constellation map of one of the nine original SQAM signals is shown in the upper part of Fig. 7. These SQAM signal is reproduced by numerical analysis and the result is shown in the lower part. The constellation map of the eight reproduced SQAM signals, excluding the reference signal, is shown in the lower right of the figure. The reproduced signal modulated to two-level amplitude and four-level phase were decoded. However, it is confirmed that the reproduced signal is dispersed for each symbol. Under the condition of small Lp, not only the spectrum of the SQAM signal spreads, but also the spectrum of the unnecessary component spreads. The unnecessary components are distributed far from the signal spectrum, but their higher order components that overlap with the signal spectrum are passed through filters. It becomes noise, which degrades the accuracy of the reproduced signal.

The Euclidean distance between the reproduced signal and the original 8 symbol values on the constellation map was calculated, and the closest symbol value was considered as the value of the reproduced signal. From the results, SER, which is the ratio of the number of signals decoded with incorrect symbol values to the total number
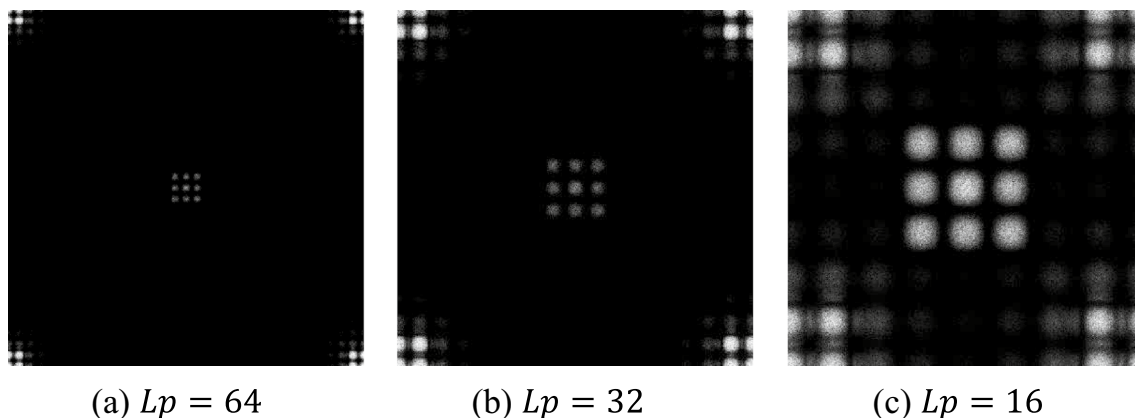

(a) $Lp = 64$ (b) $Lp = 32$ (c) $Lp = 16$

Fig. 6 Spectral distribution of 9 SQAM signals on the recording plane
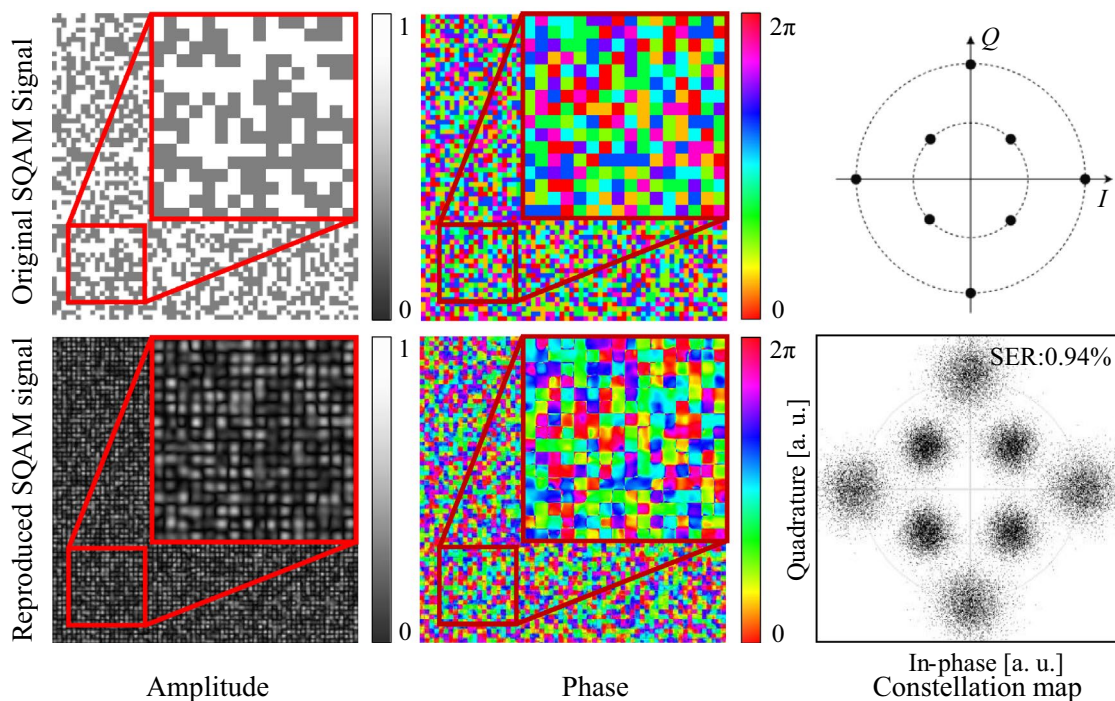
Fig. 7 Numerical results of original SQAM signals and decoded signals in case of $Lp = 16$. The upper part shows the two-level amplitude and four-level phase of one SQAM signal included in a recording page and constellation map for eight SQAM signal without the reference signal. The lower part also shows the results of the decoded signal
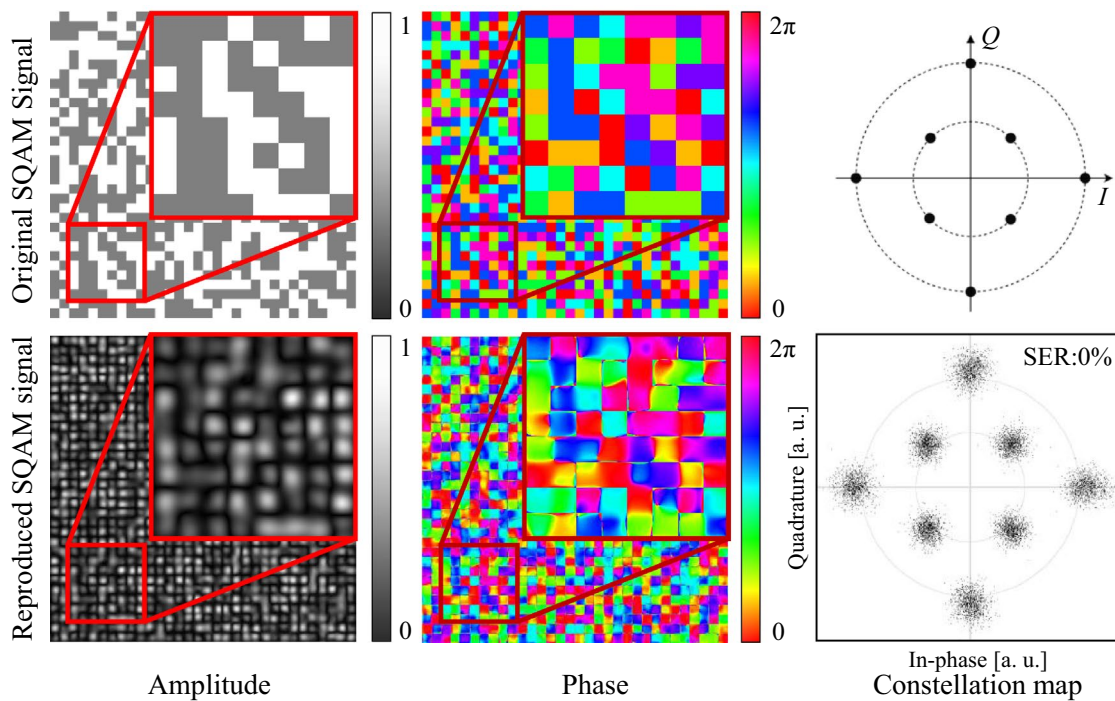

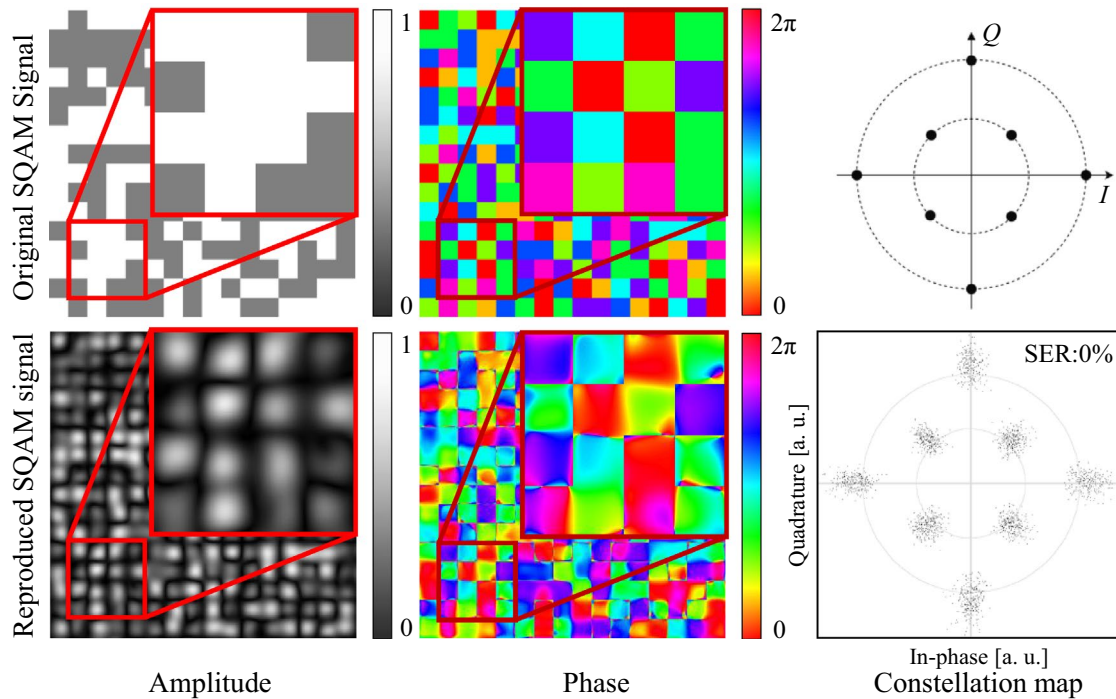**Fig. 8** Numerical results of original SQAM signals and decoded signals in case of $Lp = 32$

Fig. 9 Numerical results of original SQAM signals and decoded signals in case of $Lp = 64$
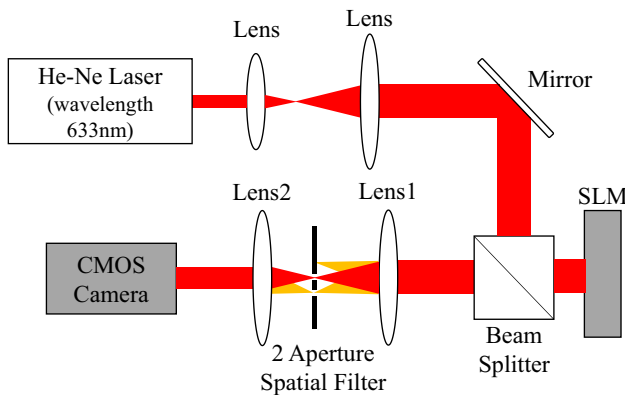
Fig. 10 Experimental setup for reproducing SQAM signals by self-interference

Table 2 Parameters for experimental setup

Multiplexed number	3
Data number i	0~2
Bit per symbol	3
Lp	16,32,64
SLM pixels	1024×1024
Pixel pitch of SLM	10.4 μm
Focal length of lens1 $f1$	300 mm
Focal length of lens2 $f2$	100 mm
Wavelength λ	633 nm

5 Experimental reproduction of SQAM signals by self-interference

We conducted a principle experiment to generate multiple SQAM page data using the interleaved phase method and to reproduce the amplitude and phase values of the SQAM signal by self-interference. The experimental setup is shown in Fig. 10. The experimental conditions are listed in Table 2. The multiplexed number SQAM signals including the reference signal was set to 3, and the size of one symbol Lp was set to 16, 32 and 64. From Eq. (23), the area of one symbol of the actual SQAM signal is $Lp\Delta x \times Lp\Delta y$, where Δx and Δy are pixel pitch of the SLM. The phase value of $P(x, y)$ was calculated from

of reproduced signals, was calculated. The degradation of the reproduced signal is caused by crosstalk of higher order components, and the average SER was 0.94% in case of $Lp = 16$.

The results for $Lp = 32$, $Lp = 64$ are shown in Figs. 8 and 9. The average SER was 0% for both cases. By setting Lp to a large value, not only the spectrum of the SQAM signal but also that of the unnecessary components become smaller, making separation easier. As a result, crosstalk can be suppressed and the quality of the reproduced signal is improved.

Eq. (4), so that the three spectra of SQAM signals were distributed at positions separated from each other by $\frac{2f\lambda}{Lp\Delta x}$ in the lateral direction on the focal plane, and the phase distribution are displayed on the SLM. The beam is expanded and guided to the SLM, where it is modulated by the SLM and focused onto the recording surface by lens1. The holographic memory is not actually recorded here. Instead, the beam used for recording is considered to be a reproduction beam generated by reference beam.

In the experiment, spherical aberration of the lens and other factors cause differences in the obtained amplitude and phase. To compensate for this effect, a reference signal with constant amplitude and phase is reproduced to obtain a complex amplitude distribution that is used to correct for aberration. Note that the bundled SQAM signal synthesized on the SLM have the same phase distortion because they are generated by the same SLM. Therefore, once the calibration wavefront is measured, it can be used to correct the wavefront of all SQAM signals.

The phase-modulated light with the phase distribution corresponding to $P(x, y)$ was generated by SLM and Fourier transformed by a lens. A plastic plate was inserted with a hole whose size was adjusted to pass only two SQAM signal components. The spatial filter blocked the unnecessary components and one of the SQAM signals. Another

component of the SQAM signal and a self-reference signal were transmitted through the filter, and the interference intensity distribution of these two lights was obtained by a camera. Fourier fringe analysis was applied to the distribution to obtain a complex amplitude distribution. From this complex amplitude distribution, the reconstructed SQAM signal was calculated by removing the already measured distortion.

One of the reconstructed SQAM signals is shown in Figs. 11, 12 and 13. The SER of $Lp = 16$ was 2.6%. The SER of $Lp = 32, 64$ were 0% for both cases. For $Lp = 16$, the SER increased compared to the numerical analysis. This result implies that increasing Lp reduces both of spread of the signal and unnecessary spectrum, thus reducing crosstalk. This is similar to results of numerical analysis in the Sect. 4.

6 Numerical analysis of reproduction accuracy for multiplexed number

In the proposed method, as the number of multiplexes increases, the recording area of the signal component becomes larger and separation of it from the unnecessary components becomes more difficult. To clarify this, the reproduction accuracy was analyzed when the multiplexed number of SQAM signals was set from 9 to 120. The size
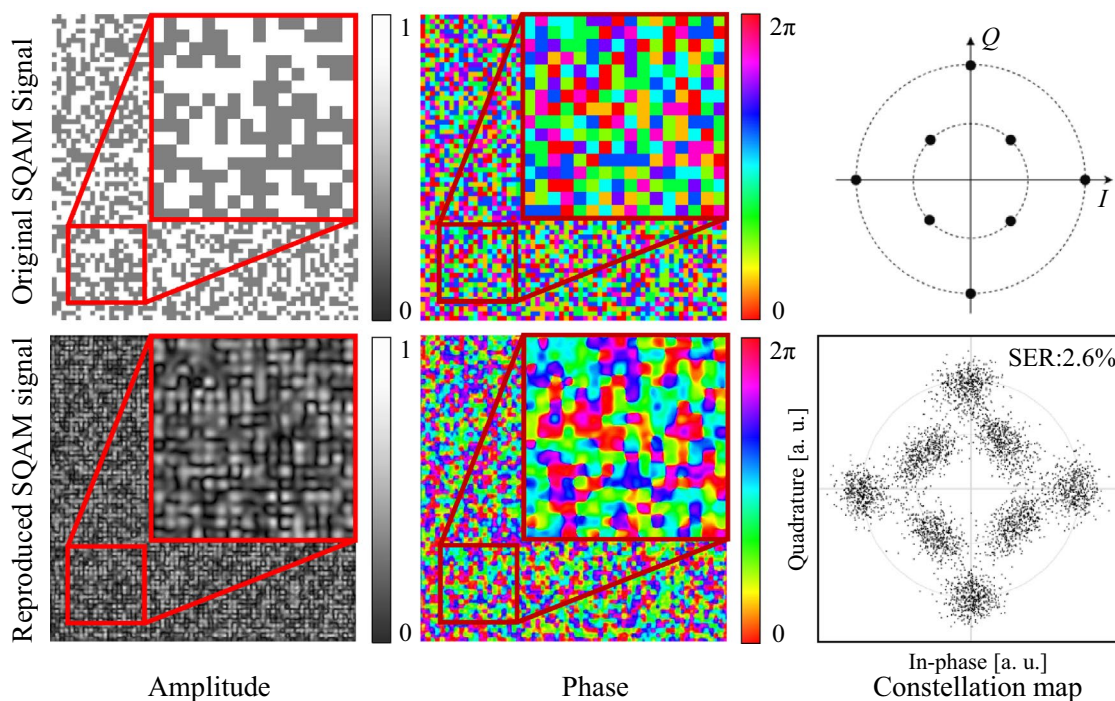

Fig. 11 Experimental results of original SQAM signals and decoded signals at $Lp = 16$. The upper part shows the two-level amplitude and four-level phase of a SQAM signal included in a recording page, and constellation map for eight SQAM signal without the reference signal. The lower part also shows the results of the decoded signal
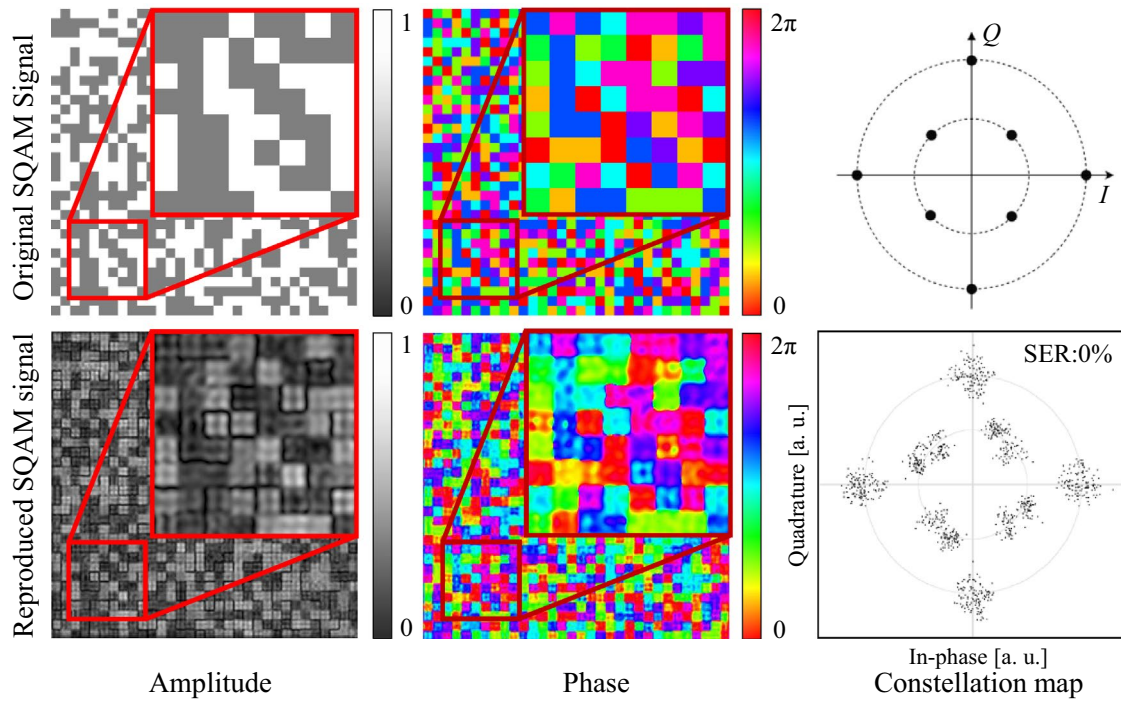
Fig. 12 Experimental results of original SQAM signals and decoded signals in case of $Lp = 32$
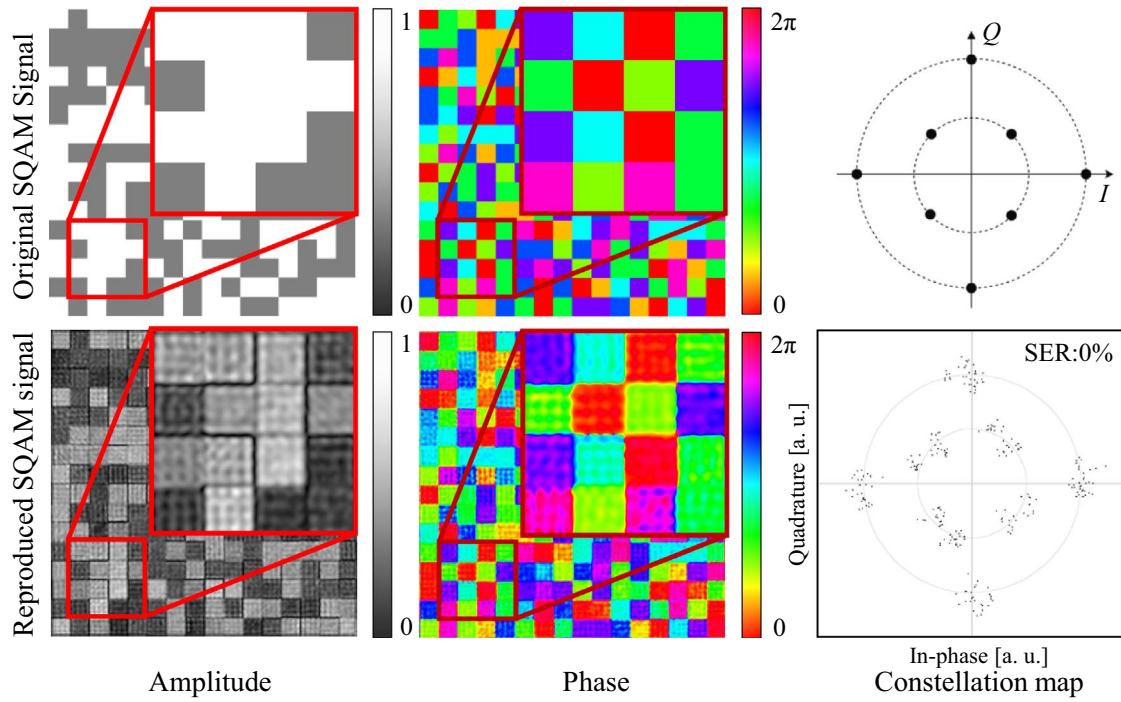

Fig. 13 Experimental results of original SQAM signals and decoded signals in case of $Lp = 64$

of a symbol Lp was set to 32. The intensity distribution of the focal plane when the multiplexed number was set to 15, 60, and 120 is shown in Fig. 14. As shown in the figure, the spectrum of each SQAM signal D_i was aligned horizontally on the focal plane.
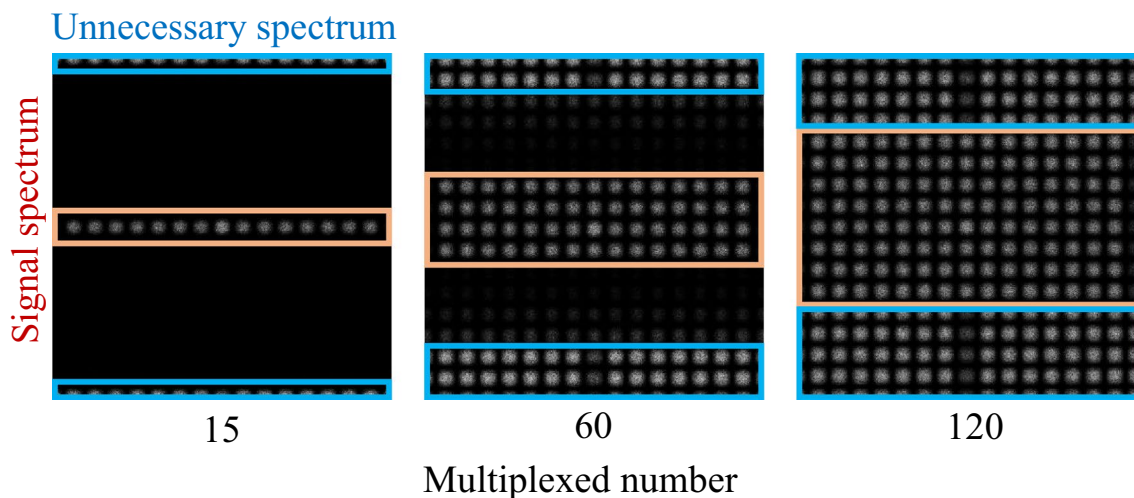
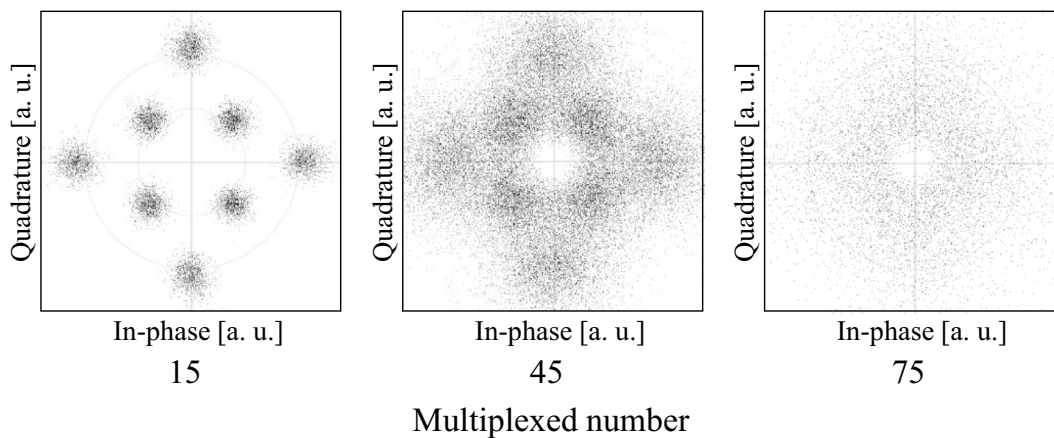**Fig. 14** Multi-column spectral distribution of SQAM signals and unnecessary component

Fig. 15 Constellation maps of decoded SQAM signal against multiple number of SQAM signal included in a recording page
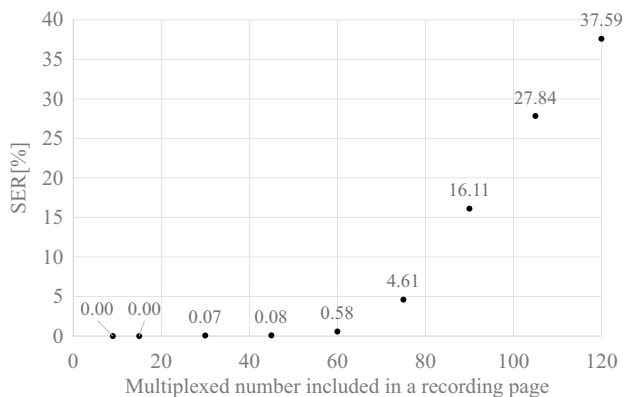

Fig. 16 Symbol error rate of decoded SQAM signals against multiple number of SQAM signal included in a recording page

A constellation map of the analysis results is shown in Fig. 15. As the number of multiplexes increases, the complex amplitude values are further distorted from the original data. As shown in Fig. 16, when the number of multiplexes is 75 or more, the average SER is more than 4%. The reason for this increase in SER is the effect of the higher order spectrums of the unnecessary components spreading around the signal components, as clearly shown in Figs. 2 and 14. The distance between the unnecessary spectrum and the signal spectrum becoming closer as the number of multiplexes increases, and the signal spectrum is affected by the unnecessary spectrum. According to the results in Fig. 16, this effect can be avoided by choosing the multiplex number and the aperture size of the spatial

filter appropriately. By setting the multiplex number to 60, SER is less than 1%, and it is possible to record and reconstruct SQAM signals. It is also not always necessary to increase the multiplex number of SQAM signal in a page data. This is because although the amount of information recorded in a single recording operation decreases as the number decreases, the actual recording density does not change because the exposure area on the holographic memory used for recording also decreases.

7 Conclusion

In this paper, we proposed a method for decoding complex amplitude signals using self-referencing and gave a hologram recording scheme suitable for this method. In the recording process, multiple SQAM signals with different linear phase codes were generated by the spatial light modulator and recorded batchwise into the holographic memory. On the recording medium, the spectrums of the SQAM signals were spatially split and arranged so as not to overlap. The spectral distributions of the unnecessary components paired at distant positions were also similarly arranged. A spatial filter shut the main component of the unnecessary component to avoid the unwanted exposure of the media, and a hologram corresponding to the spectrums of the signal components were recorded on the recording medium. In reading and decoding process, the two SQAM signals are selectively extracted and read from the memory and the interference intensity distribution of these light. We showed that it is possible to measure the amplitude and phase value of the selected SQAM signal by applying Fourier fringe analysis to the interference intensity distribution. The interference measurement between the complex amplitude signal regenerated from holographic memory is possible without the need for a reference beam propagating through different optical paths. It is thought that the optical system is compact and has high robustness against external vibrations and phase perturbations caused by air.

We extracted two SQAM signals from a page data consist of 9 SQAM signals and evaluated the decoding accuracy by numerical analysis. It was found that the smaller the number of SLM pixels used for 1 symbol of SQAM signal, the slightly lower the decoding accuracy. When the recording signal is generated by the interleaved phase method, the spectrum of the SQAM signal and the spectrum of the unnecessary component are distributed at distant positions. If the number of pixels is set to be small, the spread of the spectrum distribution becomes large, and the influence of deterioration of the reproduced signal due to crosstalk becomes strong. In this paper, we conducted a principle experiment and showed that a similar tendency appeared.

In the end, we evaluated symbol error rate against the number of SQAM signals used in a recording process. It was shown that it becomes difficult to spatially separate the spectrum of the signal light and the unnecessary component during recording, and the deterioration of the decoding accuracy due to crosstalk increases when the number of SQAM signals composing the page data is set large. Therefore, it is not appropriate to bundle too many SQAM signals into one page data. This means that the amount of data that can be recorded at one time is limited. However, note that the exposure area used to record the hologram also becomes smaller when we reduce the number of multiple SQAM signal. In other words, even if the amount of information recorded at one time is reduced, the area of the medium used for recording is reduced, so there is no change in the effective information recording density.

In the demonstration experiment, a plastic plate was inserted with a hole whose size was adjusted to pass only two SQAM signal components, so that the position of the aperture is fixed. We have not fully explained how to dynamically control the positions of the two apertures. In practical case, we have to use the spatial light modulator for control of the position of the two apertures. As an alternative method, we are considering decoding by preparing a fixed aperture for reading two adjacent holograms and manipulating it laterally. In that case, it is only necessary to prepare a known reference SQAM signal in the first reconstruction step. In subsequent steps, the decoded SQAM signal can be used to decode the adjacent signals.

This paper presented the principal analysis and experimental results of measuring the complex amplitude values of SQAM signals by generating multiple SQAM signals and selectively extracting them. If the hologram is recorded in an actual holographic memory, the accuracy of the signal reconstructed from the hologram should be affected by medium parameters such as medium thickness, saturation, and nonlinearity of refractive index change. Therefore, in the future, it is necessary to conduct an analysis that considers the above parameters. We also plan to conduct experiments using photopolymers.

References

1. Hilbert, M., López, P.: The world's technological capacity to store, communicate, and compute information. Science **332**, 60–65 (2011)
2. D. Reinsel, J. Gantz, J. Rydning: The evolution of data to life-critical, An IDC White Paper. 1–25 (2017).

3. Jones, N.: How to stop data centres from gobbling up the world's electricity. Nature **561**, 163–166 (2018)

4. Gu, M., Li, X., Cao, Y.: Optical storage arrays: a perspective for future big data storage, Light. Sci. Appl. **3**, e177 (2014)

5. Curtis, K., Dhar, L., Hill, A., Wilson, W., Ayres, M.: Holographic data storage: from theory to practical systems. Wiley (2010)

6. Liu, J., Horimai, H., Lin, X., Huang, Y., Tan, X.: Phase modulated high density collinear holographic data storage system with phase-retrieval reference beam locking and orthogonal reference encoding. Opt. Express. **26**(4), 3828–3838 (2018)

7. Kuroda, K., Matsuhashi, Y., Fujimura, R., Shimura, T.: Theory of polarization holography. Opt. Rev. **18**(5), 374–382 (2011)

8. M. Bunsen, S. Umetsu, M. Takabayashi and A. Okamoto: (2013) Method of Phase and Amplitude Modulation/Demodulation Using Datapages with Embedded Phase-Shift for Holographic Data Storage, JJAP, 52, 09LD04

9. Shibukawa, A., Okamoto, A., Takabayashi, M., Tomita, A.: Spatial cross modulation method using a random diffuser and phase-only spatial light modulator for constructing arbitrary complex fields. Opt. Express **22**(4), 3968–3982 (2014)

10. Neto, G., Roberge, D., Sheng, Y.: Full-range, continuous, complex modulation by the use of two coupled-mode liquid-crystal televisions. Appl. Opt. **35**(23), 4567–4576 (1996)

11. Shibukawa, A., Okamoto, A., Goto, Y., Honma, S., Tomita, A.: Digital phase conjugate mirror by parallel arrangement of two phase-only spatial light modulators. Opt. Express **22**, 11918–11929 (2014)

12. Nobukawa, T., Nomura, T.: Multilevel recording of complex amplitude data pages in a holographic data storage system using digital holography. Opt. Express **18**, 21001–21011 (2016)

13. Nobukawa, T., Nomura, T.: Correlation-based multiplexing of complex amplitude data pages in a holographic storage system using digital holographic techniques. Polymers (Basel). **9**(8), 375–388 (2017)

14. Honma, S., Sekiguchi, T.: Multilevel phase and amplitude modulation method for holographic memories with programmable phase modulator. Opt. Rev. **21**(5), 597–598 (2014)

15. S. Honma and H. Funakoshi: A two-step exposure method with interleaved phase pages for recording of SQAM signal in holographic memory, JJAP, 58, SKKD05 (2019)

16. S. Honma, H. Watanabe and Y. Nakajima: A recording method for SQAM signal in holographic memories and improvement of areal information density, ISOM'20 Technical Digest, We-D-03 (2020)

17. Okamoto, A., Kunori, K., Takabayashi, M., Tomita, A., Sato, K.: Holographic diversity interferometry for optical storage. Opt. Express. **19**(14), 13436–13444 (2011)

18. Nobukawa, T., Muroi, T., Katano, Y., Kinoshita, N., Ishii, N.: Single-shot phase-shifting incoherent digital holography with multiplexed checkerboard phase gratings. Opt. Lett. **43**(8), 1698–1701 (2018)

19. Bunsen, M., Tateyama, S.: Detection method for the complex amplitude of a signal beam with intensity and phase modulation using the transport of intensity equation for holographic data storage. Opt. Express **27**(17), 24029–24042 (2019)

20. Allen, L.J., Oxley, M.P.: Phase retrieval from series of images obtained by defocus variation. Opt. Comm. **199**, 65–75 (2001)

21. Kemao, Q.: Applications of windowed Fourier fringe analysis in optical measurement: a review. Opt. Lasers Eing. **66**, 67–73 (2015)